

Combinatorial Chemistry | Hot Paper |

Photochemical “In-Air” Combinatorial Discovery of Antimicrobial Co-polymers

Sarah-Jane Richards,^[a] Adam Jones,^[a] Ruben M. F. Tomás,^[a] and Matthew I. Gibson*^[a, b]

Abstract: There is an urgent need to identify new, non-traditional antimicrobials. The discovery of new polymeric antimicrobials is limited by current low-throughput synthetic tools, which means that limited chemical space has been explored. Herein, we employ photochemical “in-air” reversible addition–fragmentation chain-transfer (RAFT) polymerization with microwell plates, using liquid-handling robots to assemble large libraries of cationic polymers, without the need for degassing or purification steps, facilitating transfer to screening. Several lead polymers were identified including a co-polymer with propylene glycol side chains with significantly enhanced antimicrobial activity and increased therapeutic window. Mechanistic studies showed that this polymer was bacteriostatic, and surprisingly did not lyse the cell membranes, implying an alternative mode of action. This versatile method using simple robotics will help to develop new biomaterials with emergent properties.

Combinatorial methods are widely employed in small-molecule chemistry to identify previously unknown leads against well-characterized targets, and includes concepts, such as fragment-based design.^[1,2] Commercial compound libraries are available with >5000 members, and repurposing of known drugs is underpinned by screening.^[3] In the discovery of polymer biomaterials, there are the additional variables of monomer, molecular weight, and architecture. This provides vast chemical space to be explored, presenting a challenge and opportunity.^[4] Polymers for gene delivery have been successfully identified using combinatorial condensation polymerization,^[5,6]

but there was molecular-weight heterogeneity. Alexander et al. have developed automated high-throughput screens for polymer surfaces enabling discovery of polymer surfaces for resisting bacterial attachment^[7] or the culture of stem cells.^[8] However, for soluble polymers intended to interface with cells/proteins, well-defined materials are required with control of M_w to enable selection and tuning of the final properties.^[9,10] Controlled radical (CRP) or ionic polymerization requires inert atmospheres and sealed vials, and in the case of ionic polymerizations—rigorously anhydrous conditions, adding complexity and time due to processing. Schubert and co-workers have used automated synthesizers for polymerizations, but such protocols require a precipitation/isolation step limiting the potential of the libraries.^[4,11] To truly use combinatorial polymer methods to discover “drug-like” materials, the synthetic and handling methods should be compatible with the industry standard, 96-, 384-, and 1536-well plates used in biomedical screening with liquid-handling robotics.^[12]

To address the combinatorial challenge, air-tolerant CRP methods are emerging. Chapman et al. used glucose oxidase for in situ degassing in 96-well plate format reversible addition–fragmentation chain-transfer (RAFT) polymerizations,^[13] and this approach has also been applied to ATRP formulations.^[14] Light-mediated polymerizations^[15] enable the trapping/removal of oxygen species by using organic^[16] and inorganic^[17] photoredox catalysts. Trithiocarbonates can also be used as intrinsic photoredox catalysts in RAFT, without the need for supplemental catalysts which is appealing for biomedical screening.^[18] Recently, Boyer and co-workers used photo-RAFT in 96-well plates to screen star polymers for binding to a model lectin, facilitating the design of new binders.^[19] However, there are limited examples of application to urgent biomedical materials screening challenges, such as new antimicrobials to combat resistance.^[20] Cationic polymers have been employed as antimicrobial agents, inspired by antimicrobial peptides^[21] with broad spectrum activity and slow emerging resistance.^[22] The most active antimicrobial polymers are not homopolymers, but require a complex balance of charge and hydrophobicity/-philicity by incorporation of co-monomers.^[23–26] Their rational design is typically based on targeting membrane lysis, but it is becoming apparent that bacteria aggregation and hence interruption of signaling^[27,28] pore-formation,^[29] DNA-binding,^[30] and interrupting metabolic processes^[31] are associated with polycations. Structure–function maps to phenotype (bacteria killing), but also to understand mechanism, are needed to generate data sets to enable ab initio materials design.^[7]

[a] Dr. S.-J. Richards, A. Jones, R. M. F. Tomás, Prof. M. I. Gibson
Department of Chemistry
University of Warwick, Gibbet Hill Road, Coventry, CV47AL (UK)
E-mail: m.i.gibson@warwick.ac.uk

[b] Prof. M. I. Gibson
Warwick Medical School, University of Warwick, CV4 7AL (UK)

Supporting information and the ORCID identification number(s) for the author(s) of this article can be found under:

<https://doi.org/10.1002/chem.201802594>. It contains the Experimental Section, in which synthetic procedures, characterization, microbiology, and cell-culture manipulations are described.

© 2018 The Authors. Published by Wiley-VCH Verlag GmbH & Co. KGaA. This is an open access article under the terms of Creative Commons Attribution NonCommercial License, which permits use, distribution and reproduction in any medium, provided the original work is properly cited and is not used for commercial purposes.

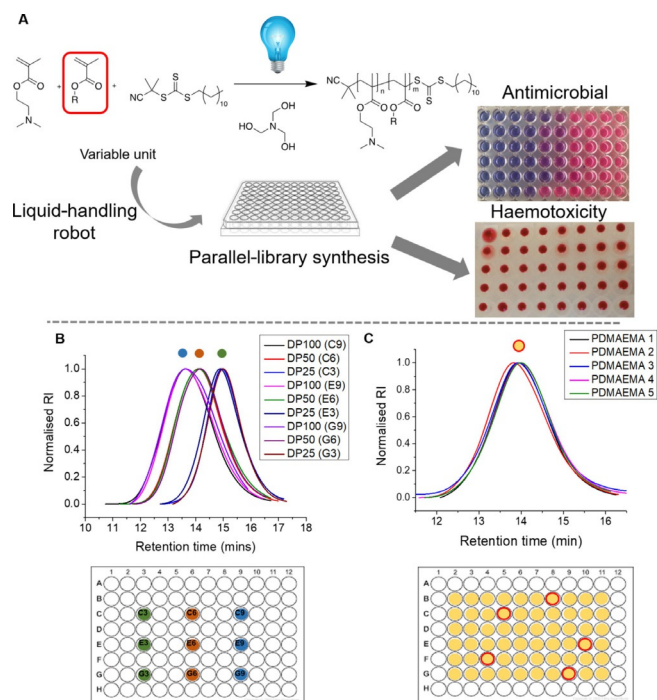


Figure 1. A) Concept of in-air combinatorial photo-RAFT discovery. B) SEC of 3×3 DP polymerizations of DMAEMA. C) SEC of five randomly selected (red circles) polymers produced from 60×DMAEMA polymerizations within a single plate.

Herein, we present combinatorial cationic photopolymer screening for new antimicrobial biomaterials. The intrinsic photo-RAFT method^[18] is adapted to enable automation, scalability and ease of use in “open” reaction vessels of a 96 well plate, using liquid handling robots, Figure 1A. A photo-RAFT agent 2-cyano-2-propyl dodecylthiocarbonate is used with a tertiary amine (triethanolamine (TEOA)), to degas the solvent (DMSO) enabling polymerization to proceed under a blue LED light. 2-(Dimethylamino)ethyl methacrylate (DMAEMA) was chosen as the cationic component based on our previous work showing it has potent anti-mycobacterial activity. Herein, there did not appear to be a molecular-weight effect of the DPs tested (between 10 and 100) therefore DP 75 was chosen.^[32,33] Figure 1B and Table 1 show results of three parallel DMAEMA polymerizations in 96-well plates targeting degrees of polymerization of 25, 50, and 100. Each achieved >95% conversion and comparable molecular-weight distributions confirming reproducible synthesis in the small reaction volumes (<200 μL). The procedure was validated further by running 60 parallel in-air polymerizations of DMAEMA within a single plate. Five wells were then chosen by an independent party for SEC analysis, Figure 1C. Comparable molecular weights and distributions were obtained, confirming control over the reaction and homogeneity across all the mini-reaction vessels (wells).

Traditional polymerization methods are limited in their chemical and compositional space meaning the “sweet spots” in co-polymer libraries can be overlooked. Here, eight co-monomers were chosen to be co-polymerized with DMAEMA, including a mixture of hydrophobic and hydrophilic substituents, at four densities (5, 10, 15, 20 mol%) with three repeats,

Well code	[M]: [CTA]	Conv. [%] ^[a]	$M_n(\text{theor})$ [g mol ⁻¹] ^[b]	$M_n(\text{SEC})$ [g mol ⁻¹] ^[c]	M_w/M_n ^[c]
C3	100	95	15 300	22 900	1.66
C6	50	96	7900	17 200	1.57
C9	25	98	4200	9500	1.33
E3	100	96	15 400	22 100	1.63
E6	50	95	7800	16 800	1.60
E9	25	95	4100	9900	1.37
G3	100	96	15 400	23 200	1.61
G6	50	97	8000	17 300	1.49
G9	25	98	4200	9400	1.33

[a] Determined by ¹H NMR analysis against an internal mesitylene standard. [b] Determined by the [M]:[CTA] ratio and conversion, assuming 100% CTA efficiency. [c] Determined by SEC in DMF; reported values are relative to PMMA standards.

within 96-well plates to give a combinatorial library of 108 distinct polymers in DMSO, Figure 2 (left column) prepared in a single day. Drug screening was routinely conducted in 1–5% DMSO to aid solubilization;^[34] herein, sampling followed by dilution in appropriate buffer/media resulted in [DMSO] <5 wt%, which controls showed did not affect assays.

A series of functional screens were undertaken and results indicated as a heat map (Figure 2; green indicates desirable

Structural/Compositional Diversity	mol% Co-monomer	Toxicity			Selection of Hits			Hit?	Lead Identification
		Haemolytic at 1 mg.mL ⁻¹			MIC ₉₉ <125 μg.mL ⁻¹				
		1	2	3	1	2	3		
MMA	5	Green	Green	Green	Red	Red	Red	×	
	10	Green	Green	Green	Red	Red	Red	×	
	15	Green	Green	Green	Red	Red	Red	✓	250
	20	Green	Green	Green	Red	Red	Red	✓	500
EMA	5	Green	Green	Green	Red	Red	Red	×	
	10	Green	Green	Green	Red	Red	Red	×	
	15	Green	Green	Green	Red	Red	Red	✓	250
	20	Green	Green	Green	Red	Red	Red	✓	250
iPMA	5	Green	Green	Green	Red	Red	Red	×	
	10	Green	Green	Green	Red	Red	Red	×	
	15	Green	Green	Green	Red	Red	Red	✓	125
	20	Green	Green	Green	Red	Red	Red	×	
cHMA	5	Green	Green	Green	Red	Red	Red	✓	125
	10	Green	Green	Green	Red	Red	Red	✓	125
	15	Green	Green	Green	Red	Red	Red	×	
	20	Green	Green	Green	Red	Red	Red	×	
HEMA	5	Green	Green	Green	Red	Red	Red	×	
	10	Green	Green	Green	Red	Red	Red	×	
	15	Green	Green	Green	Red	Red	Red	×	
	20	Green	Green	Green	Red	Red	Red	×	
DEGMA	5	Green	Green	Green	Red	Red	Red	×	
	10	Green	Green	Green	Red	Red	Red	×	
	15	Green	Green	Green	Red	Red	Red	×	
	20	Green	Green	Green	Red	Red	Red	×	
PEGMA	5	Green	Green	Green	Red	Red	Red	×	
	10	Green	Green	Green	Red	Red	Red	×	
	15	Green	Green	Green	Red	Red	Red	×	
	20	Green	Green	Green	Red	Red	Red	×	
PPGMA	5	Green	Green	Green	Red	Red	Red	✓	62.5
	10	Green	Green	Green	Red	Red	Red	✓	62.5
	15	Green	Green	Green	Red	Red	Red	✓	15.6
	20	Green	Green	Green	Red	Red	Red	✓	31.3

Figure 2. Library structure, haemolysis at 1 mg mL⁻¹ and antimicrobial activity against *E. coli* at 125 μg mL⁻¹ (0.5 × MIC₉₉ of homopolymer (PDMAEMA)).

outcome, red indicates sample is excluded). To eliminate toxic materials, ovine red blood cell haemolysis was conducted at 1 mg mL^{-1} (Figure 1A). All 108 polymers had haemolysis below 2% and no haemagglutination, hence all passed. To screen for antimicrobial activity, the resazurin reduction assay was used, which gives a colorimetric output (blue to pink, Figure 1A). *Escherichia coli* and *Mycobacteria smegmatis* were used to represent Gram negative and Mycobacteria (which includes *M. tuberculosis*). The MIC_{99} (minimum concentration to stop growth of 99% of organisms) of homo-PDMAEMA is 250 and $31.3 \text{ } \mu\text{g mL}^{-1}$ against *E. coli* and *M. smegmatis*, respectively.^[32,33] Co-polymers were added to the bacteria at $0.5 \times \text{MIC}_{99}$ of PDMAEMA to enable selection of co-polymers that were at least two-fold more active. Against *M. smegmatis*, there were few "hits", potentially due to the complex mycobacterial cell walls, which are rich in mycolic acids and glycans which can "shield" the membrane.^[32] However, the *E. coli* screen identified several "hits" with co-polymers of MMA, iPMA, cHMA, and PPGMA inhibiting *E. coli* growth at $0.5 \times \text{MIC}_{99}$ of the parent homopolymer.

These hits were tested across a wider concentration range to establish their MIC_{99} (Figure 2, right column). Hydrophobic co-monomers tended to lower the MIC_{99} . MMA co-polymers had a sweet spot for activity at 15 wt% with more/less reducing all antimicrobial activity. Similarly, iPMA/cHMA co-polymers were active at 5 and 10 wt% but not at higher incorporation levels. Several of the hits appeared to not give lower MIC_{99} values than the homopolymer once tested in full dilution series, justifying the hit-to-lead approach. These observations highlight a key benefit of screening to identify non-linear trends that can be missed in low-throughput testing. The most active co-polymer contained 15 wt% poly(propylene glycol)methacrylate (PPGMA) with an MIC_{99} of $15 \text{ } \mu\text{g mL}^{-1}$, compared to $250 \text{ } \mu\text{g mL}^{-1}$ for homo-PDMAEMA. Interestingly, this is not the most hydrophobic comonomer (see $\log P$ values in the Supporting Information) suggesting that a membrane insertion/disruption mechanism might not be operating. This would not have been predicted based on $\log P$ values alone.

To validate these findings, P(DMAEMA(85%)-co-PPGMA(15%)) hits were resynthesized to various degrees of polymerization (DP30-240) to give a panel of "pure", well-defined polymers (SEC traces, Figure 3A). Similar MIC_{99} values were obtained as in the initial screen, but the shortest polymers (DP30) were identified to be least active, Figure 3B. Membrane-integrity assays were undertaken to probe the for the greater co-polymer activity compared to PDMAEMA homopolymer; it is assumed that more hydrophobic units promotes insertion into bacterial cell membranes, leading to lysis and cell death.^[24] The assay employs a pair of dyes, SYTO 9 (green fluorescence) that enters all cells and is associated with intact bacteria and propidium iodide (red fluorescence) that can only enter membrane-compromised cells to probe if membrane lysis has occurred. Figure 3C–H shows confocal microscopy images of *E. coli* incubated under various conditions. PDMAEMA at $2 \times \text{MIC}_{99}$ shows only red bacteria, consistent with the "dead" control (Figure 3D) and at $0.5 \times \text{MIC}_{99}$ a mixture of red/green are seen supportive of PDMAEMA homopolymers killing *E. coli* by a lytic mechanism. However, P(DMAEMA(85%)-co-PPGMA(15%)) at a concentra-

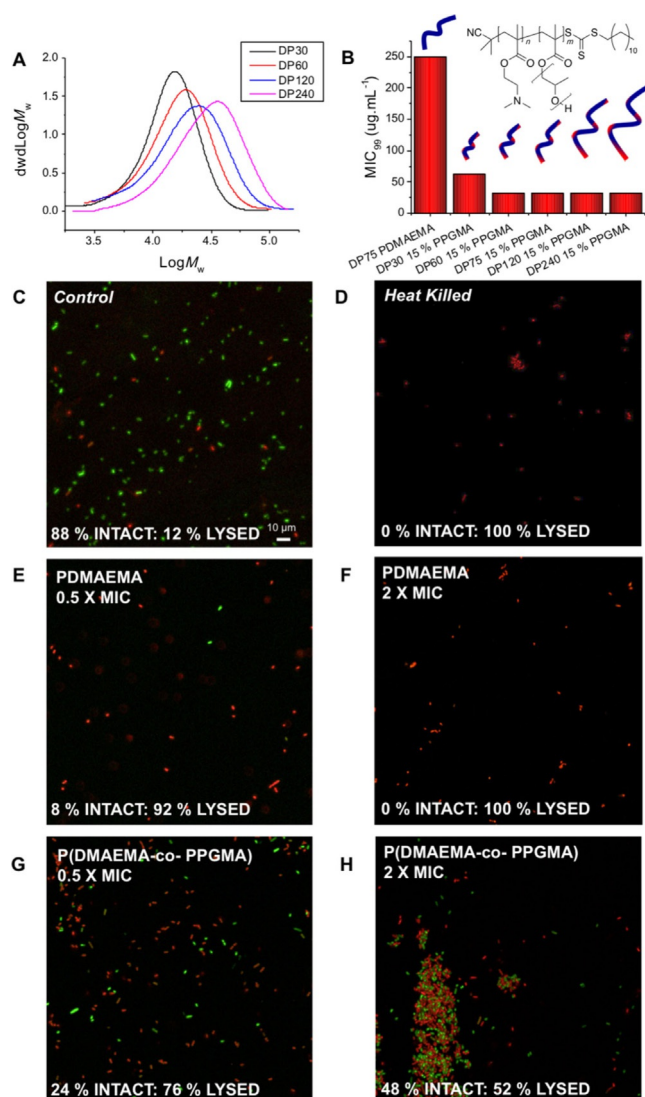


Figure 3. A) SEC of P(DMAEMA(85%)-co-PPGMA(15%)) co-polymers. B) MIC_{99} of PDMAEMA compared to P(DMAEMA(85%)-co-PPGMA(15%)) co-polymers. C–H) Fluorescence microscopy of *E. coli* upon exposure to varying concentrations of PDMAEMA and P(DMAEMA(85%)-co-PPGMA(15%)). Green channel shows intact membranes, red is damaged membranes.

tion above ($2 \times$) MIC_{99} gave a mixture of red and green bacteria, showing that there is less membrane lysis than the PDMAEMA homopolymers even though these are more active (lower MIC_{99}). This shows that the co-monomer is not simply increasing activity by more membrane lysis. Confocal microscopy suggested increased bacterial aggregation in response to the co-polymer, but not the homopolymer. Aggregation is known to modulate bacterial responses in their environment, and the co-polymers might be influencing their colonizing behaviour to limit growth by a feedback mechanism.^[27,35]

To determine if the bacteria were being killed by the co-polymers, or if their growth was being inhibited, the minimum bactericidal concentration (MBC) was determined. For PDMAEMA homopolymers, the MBC is the same as the MIC_{99} suggesting membrane lysis is the mode of action as would be expected for traditional cationic polymers. For the co-polymer, the MBC actually increased to $> 1000 \text{ } \mu\text{g mL}^{-1}$, showing it was less

effective at killing and lysing bacteria membranes than the homopolymer. This suggested that we have identified a mechanism, in which a unique co-polymer that inhibits *E. coli* growth potentially due to aggregation was detected, and not physical damage of the cell membrane. Bactericidal and bacteriostatic mechanisms are both valid in terms of antimicrobial therapy with front lines drugs having one or both of these properties.^[36] The polymers were also evaluated for cytotoxicity against a mammalian cell line (A549; see the Supporting Information). Incorporation of PPGMA co-monomers slightly decreased cell viability relative to the PDMAEMA after 24 hours. However, due to the increased antimicrobial activity, the PPGMA co-polymers have a larger window of activity.

In summary, we have developed a rapid, scalable, and simple approach to identify emergent antimicrobial properties of co-polymer libraries through the use of in-air polymerization coupled to liquid-handling robots in 96-well plates. A screening and selection process enabled identification of hits within a 108-member co-polymer library resulting in co-polymers of oligo(propylene glycol) being identified with 16-fold increased activity compared to PDMAEMA homopolymers. Crucially, PPGMA was not the most hydrophobic co-monomer tested, and non-linear relationships were observed between co-monomer composition and activity. This material was shown to have a distinct mechanism of action, inhibiting bacterial growth rather than lysing the cell membranes. Such a material would not have been identified by using conventional 1-vial/1-polymer methods; furthermore, this process accelerates the discovery of new complex materials with emergent biological interactions.

Acknowledgements

We are grateful for the polymer characterization RTP for size-exclusion chromatography. M.I.G. holds an ERC Starter Grant (CRYOMAT 638661). EPSRC are thanked for studentship for R.T. (EP/L015307/1) and also INTEGRATE (EP/M027503/1). The microscopy facilities are funded by UoW Advanced Bioluminescence Research Technology Platform BBSRC ALERT14 award BB/M01228X/1. I. Galpin is acknowledged for assistance with confocal microscopy.

Conflict of interest

The authors declare no conflict of interest.

Keywords: antimicrobials · bacteria · biomaterials · combinatorial chemistry · polymers

- [1] C. W. Murray, D. C. Rees, *Nat. Chem.* **2009**, *1*, 187–192.
- [2] J. P. Kennedy, L. Williams, T. M. Bridges, R. N. Daniels, D. Weaver, C. W. Lindsley, *J. Comb. Chem.* **2008**, *10*, 345–354.
- [3] T. T. Ashburn, K. B. Thor, *Nat. Rev. Drug Discovery* **2004**, *3*, 673–683.
- [4] M. A. R. Meier, R. Hoogenboom, U. S. Schubert, *Macromol. Rapid Commun.* **2004**, *25*, 21–33.
- [5] S. Brocchini, K. James, V. Tangpasuthadol, J. Kohn, *J. Am. Chem. Soc.* **1997**, *119*, 4553–4554.
- [6] D. M. Lynn, D. G. Anderson, D. Putnam, R. Langer, *J. Am. Chem. Soc.* **2001**, *123*, 8155–8156.

- [7] A. L. Hook, C. Y. Chang, J. Yang, J. Lockett, A. Cockayne, S. Atkinson, Y. Mei, R. Bayston, D. J. Irvine, R. Langer, D. G. Anderson, P. Williams, M. C. Davies, M. R. Alexander, *Nat. Biotechnol.* **2012**, *30*, 868–875.
- [8] Y. Mei, K. Saha, S. R. Bogatyrev, J. Yang, A. L. Hook, Z. I. Kalcioğlu, S. W. Cho, M. Mitalipova, N. Pyzocha, F. Rojas, K. J. Van Vliet, M. C. Davies, M. R. Alexander, R. Langer, R. Jaenisch, D. G. Anderson, *Nat. Mater.* **2010**, *9*, 768–778.
- [9] C. Boyer, V. Bulmus, T. P. Davis, V. Ladmiraal, J. Liu, S. Perrier, *Chem. Rev.* **2009**, *109*, 5402–5436.
- [10] I. Cobo, M. Li, B. S. Sumerlin, S. Perrier, *Nat. Mater.* **2015**, *14*, 143–159.
- [11] C. R. Becer, S. Hahn, M. W. M. Fijten, H. M. L. Thijs, R. Hoogenboom, U. S. Schubert, *J. Polym. Sci. Part A* **2008**, *46*, 7138–7147.
- [12] R. MacArron, M. N. Banks, D. Bojanic, D. J. Burns, D. A. Cirovic, T. Garayantes, D. V. S. Green, R. P. Hertzberg, W. P. Janzen, J. W. Paslay, U. Schopfer, G. S. Sittampalam, *Nat. Rev. Drug Discovery* **2011**, *10*, 188–195.
- [13] R. Chapman, A. J. Gormley, M. H. Stenzel, M. M. Stevens, *Angew. Chem. Int. Ed.* **2016**, *55*, 4500–4503; *Angew. Chem.* **2016**, *128*, 4576–4579.
- [14] A. E. Enciso, L. Fu, A. J. Russell, K. Matyjaszewski, *Angew. Chem. Int. Ed.* **2018**, *57*, 933–936; *Angew. Chem.* **2018**, *130*, 945–948.
- [15] M. Chen, M. Zhong, J. A. Johnson, *Chem. Rev.* **2016**, *116*, 10167–10211.
- [16] J. Xu, S. Shanmugam, H. T. Duong, C. Boyer, *Polym. Chem.* **2015**, *6*, 5615–5624.
- [17] N. Corrigan, D. Rosli, J. W. J. Jones, J. Xu, C. Boyer, *Macromolecules* **2016**, *49*, 6779–6789.
- [18] Q. Fu, K. Xie, T. G. McKenzie, G. G. Qiao, *Polym. Chem.* **2017**, *8*, 1519–1526.
- [19] A. J. Gormley, J. Yeow, G. Ng, Ó. Conway, C. Boyer, R. Chapman, *Angew. Chem. Int. Ed.* **2018**, *57*, 1557–1562; *Angew. Chem.* **2018**, *130*, 1573–1578.
- [20] J. O'Neill, Review on Antimicrobial Resistance: Tackling drug-resistant infections globally <https://amr-review.org>; accessed May 17, **2018**.
- [21] M.-D. Seo, H.-S. Won, J.-H. Kim, T. Mishig-Ochir, B.-J. Lee, *Molecules* **2012**, *17*, 12276–12286.
- [22] S. J. Lam, N. M. O'Brien-Simpson, N. Pantarat, A. Sulistio, E. H. H. Wong, Y.-Y. Chen, J. C. Lenzo, J. A. Holden, A. Blencowe, E. C. Reynolds, G. G. Qiao, *Nat. Microbiol.* **2016**, *1*, 16162.
- [23] M. F. Ilker, K. Nüsslein, G. N. Tew, E. B. Coughlin, *J. Am. Chem. Soc.* **2004**, *126*, 15870–15875.
- [24] K. Kuroda, W. F. DeGrado, *J. Am. Chem. Soc.* **2005**, *127*, 4128–4129.
- [25] K. Kuroda, G. A. Caputo, W. F. DeGrado, *Chem. Eur. J.* **2009**, *15*, 1123–1133.
- [26] G. N. Tew, D. Liu, B. Chen, R. J. Doerksen, J. Kaplan, P. J. Carroll, M. L. Klein, W. F. DeGrado, *Proc. Natl. Acad. Sci. USA* **2002**, *99*, 5110–5114.
- [27] E. Leire, S. P. Amaral, I. Louzao, K. Winzer, C. Alexander, E. Fernandez-Megia, F. Fernandez-Trillo, *Biomater. Sci.* **2016**, *4*, 998–1006.
- [28] L. T. Lui, X. Xue, C. Sui, A. Brown, D. I. Pritchard, N. Halliday, K. Winzer, S. M. Howdle, F. Fernandez-Trillo, N. Krasnogor, C. Alexander, *Nat. Chem.* **2013**, *5*, 1058–1065.
- [29] L. Yang, V. D. Gordon, D. R. Trinkle, N. W. Schmidt, M. A. Davis, C. DeVries, A. Som, J. E. Cronan, G. N. Tew, G. C. L. Wong, *Proc. Natl. Acad. Sci. USA* **2008**, *105*, 20595–20600.
- [30] A. K. Chindera, M. Mahato, A. K. Sharma, H. Horsley, K. Kloc-muniak, N. F. Kamaruzzaman, S. Kumar, A. McFarlane, J. Stach, T. Bentine, L. Good, *Sci. Rep.* **2016**, *6*, 23121.
- [31] K. A. Brogden, *Nat. Rev. Microbiol.* **2005**, *3*, 238–250.
- [32] D. J. Phillips, J. Harrison, S.-J. Richards, D. E. Mitchell, E. Tichauer, A. T. M. Hubbard, C. Guy, I. Hands-Portman, E. Fullam, M. I. Gibson, *Biomacromolecules* **2017**, *18*, 1592–1599.
- [33] S.-J. Richards, K. Isufi, L. E. Wilkins, J. Lipecki, E. Fullam, M. I. Gibson, *Biomacromolecules* **2018**, *19*, 256–264.
- [34] J. Maes, L. Verlooy, O. E. Buenafe, P. A. M. de Witte, C. V. Esguerra, A. D. Crawford, *PLoS One* **2012**, *7*, e43850.
- [35] I. Louzao, C. Sui, K. Winzer, F. Fernandez-Trillo, C. Alexander, *Eur. J. Pharm. Biopharm.* **2015**, *95*, 47–62, (Pt A).
- [36] J. Nemeth, G. Oesch, S. P. Kuster, *J. Antimicrob. Chemother.* **2015**, *70*, 382–395.

Manuscript received: May 23, 2018

Revised manuscript received: July 21, 2018

Accepted manuscript online: August 2, 2018

Version of record online: August 20, 2018